Zeitschrift: Eclogae Geologicae Helvetiae
Herausgeber: Schweizerische Geologische Gesellschaft
Band: 93 (2000)
Heft: 3

Artikel: The influence of tectonic structures on karst flow patterns in karstified limestones and aquitards in the Jura Mountains, Switzerland

Autor: Herold, Thilo / Jordan, Peter / Zwahlen, François

DOI: https://doi.org/10.5169/seals-168827

0012-9402/00/030349-14 $1.50 + 0.20/0
Birkhäuser Verlag, Basel, 2000

Eclogae geol. Helv. 93 (2000) 349–362

The influence of tectonic structures on karst flow patterns in karstified limestones and aquitards in the Jura Mountains, Switzerland

THILO HEROLD[1,2], PETER JORDAN[2] & FRANÇOIS ZWAHLEN[1]

Key words: Karst ground water circulation, anisotropic permeability, transpressive transtensive faults, hydraulic continuity, transmissive fracture, overlapping recharge, anticline and syncline

ZUSAMMENFASSUNG

Obwohl immer wieder davon ausgegangen wird, dass sich Karstsysteme vorzugsweise entlang tektonischer Strukturen, insbesondere Klüften und Verwerfungen, entwickeln, ergaben detaillierte Feldbeobachtungen, dass verschiedene Strukturen keinen Einfluss auf die Karstentwicklung haben oder sie gar behindern. Ziel dieser Studie ist es, Gründe für dieses unterschiedliche Verhalten aufzuzeigen und Kriterien auszuarbeiten, die Voraussagen erlauben, ob bestimmte tektonische Strukturen die Karstentwicklung begünstigen oder behindern.

Zu diesem Zweck wurden drei umfangreiche Markierversuche im östlichen Faltenjura durchgeführt. Insgesamt fanden 21 Injektionen statt, und 95 Quellen wurden auf Markierstoffe untersucht. Zusätzlich wurde das gesamte Gebiet tektonisch und hydrogeologisch detailliert untersucht. Das Untersuchungsgebiet umfasst zwei grosse Antiklinalen (Weissenstein- und Farisberg-Kette), welche im Miozän in mehreren Phasen und unter spröden Bedingungen gebildet wurden. Dabei wurden die schief zu den Faltenachsen liegenden, präexistenten (oligozänen) Grabenbruchstrukturen in die Faltung einbezogen. Die Kalke des Doggers (Hauptrogenstein) und des Malms bilden zwei potentielle Karstaquifere, welche untereinander und gegen aussen durch schlecht bis kaum durchlässige Gesteine abgedichtet werden.

Die Untersuchungen zeigen, dass die Karstentwicklung nachhaltig von tektonischen Strukturen kontrolliert wird. Die raschen und weitreichenden Verbindungen entlang der Kreten und den Flanken der Antiklinalen können auf faltungsinduzierte Extensionsklüfte zurückgeführt werden. Die laterale Entwässerung der Antiklinalen konzentriert sich – obwohl aus hydraulischen Überlegungen eigentlich immer vorteilhafter – auf einige wenige Stellen, welche alle mit transtensiv reaktivierten oligozänen Grabenbrüchen korreliert werden können. Auf diese Bruchsysteme kann auch der an mehreren Orten und in beiden Richtungen feststellbare Wasseraustausch zwischen den beiden Aquiferen (Malm und Dogger) zurückgeführt werden. Es wird postuliert, dass verkarstete Kalzitfüllungen oder Kakirite, welche das Anschwellen der Tonminerale verhindern, diesen Transport durch die mergeligen Aquiclude ermöglichen. Entlang transpressiv aktivierter Grabenbrüche oder synorogener Überschiebungen bildeten sich offensichtlich keine Karstsysteme aus.

Es wird postuliert, dass diese Erkenntnisse auch auf andere orogen überprägten Kalkgebiete angewendet werden können: Karstsysteme entwickeln sich vorzugsweise entlang tektonischer Strukturen, welche in der letzten, der Verkarstung vorausgegangenen Deformationsphase extensiv oder transtensiv beansprucht wurden. Kompressive oder transpressive Strukturen sind indifferent oder wirken als Hindernisse für die Entwicklung von Karstsystemen.

ABSTRACT

The development of karst systems is often assumed to be related to tectonic structures, i. e. joints and faults. However, detailed studies report many of these structures to be indifferent or even obstacles to karst development. The aim of our study is to present a systematic which helps to explain or even predict whether a specific fault or joint, or a class of such structures are permeable (and therefore likely to be widened to karst conduits) or impermeable.

Therefore three extended multi-tracer experiments followed by three months of monitoring were performed at some 95 springs and streams in the Eastern Jura fold-and-thrust belt. In addition, detailed mapping of tectonic and hydrogeological structures, including sinkholes and some 600 springs, has been carried out. The study area is characterised by two large anticlines, which have been affected by pre-fold normal faulting and synorogenic folding and thrusting as well as oblique reactivation of pre-existing faults. Hydrogeologically, two karst aquifers can be distinguished, the lower Mid Jurassic Hauptrogenstein (Dogger Limestone) and the upper Late Jurassic Malm Limestone. Both karst aquifers are confined and separated from each other by impermeable layers.

This study has shown that karst development and groundwater circulation is strongly controlled by tectonic structures resulting in specific meso- to macro-scale anisotropies. Fast long distance transport along fold axes in crest and limb areas of anticlines is found to be related to extension joints resulting from synorogenic folds. Concentrated lateral drainage of water flow from anticline limbs is exclusively related to pre-orogenic normal faults, which have been transtensively reactivated during folding. The same structures are also responsible for the significant groundwater exchange between the lower (inner) and upper (outer) aquifer. This water flow, through otherwise impermeable layers, which is reported at several places and in both directions, is suspected to take place in porous calcite fault gouges or fault breccias. Transpressively reactivated normal faults and synorogenic reverse faults, on the other hand, are found to have no influence on karst development and groundwater circulation.

It is proposed that the systematic found in the Weissenstein area, i.e. that karst conduit development is mainly controlled by extensive or transtensive (reactivated) joints and faults, may also be applied to other tectonically influenced karst regions. Transpressive structures have no significant influence on karst system development and may even act as obstacles.

[1] CHYN, University of Neuchâtel, 11 rue Emile-Argand, 2007 Neuchâtel, Switzerland. E-mail: herold@imap.ch, francois.zwahlen@chyn.unine.ch,
[2] AWW - Water Management Authority, Greibenhof, Canton of Solothurn, 4509 Solothurn, Switzerland. E-mail: herold@imap.ch, peter.jordan@bd.so.ch

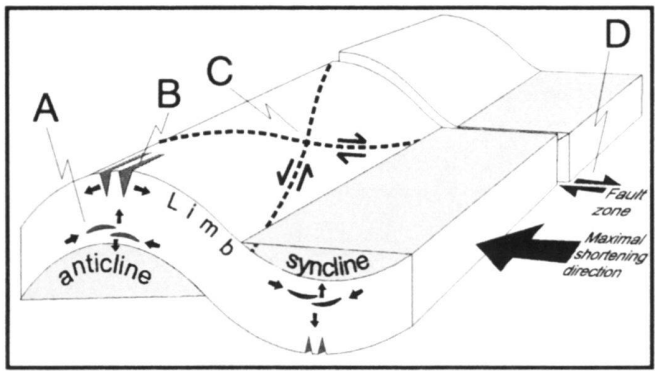

Fig. 1. Fold terminology (Ramsey & Huber 1983): As all folds in the study area are in an upward or slightly inclined position we use the more common term "anticline" in the present study. It is regarded as identical to the term "upfold" or "antiform", where the oldest rocks are present in the core. The converse applies for the term "syncline" ("synform"). The following systems can be distinguished:

A. Extension joints parallel to bedding in internal concave part of folded layers.
B. Extension joints normal to shortening direction in crest area
C. Synorogenic conjungate shear system spatial orientation is induced by maximum shortening direction and material properties
D. Reactivated prefolding normal fault with any orientation. When parallel to C), reactivation is only shearing or overthrusting, if not, reactivation consists of a shear and tensional (transtensional opening) or compressional (transpressive closing) component.

1. Introduction

The relationship between tectonic discontinuities, the orientation of cavities and the general flow direction is discussed by Kiraly (1968), Snow (1969), Kiraly et al. (1971) and Palmer (1975). The classic approach to deducing the principles of cave evolution from the observed geological structures in cave systems was highlighted by Ford and Ewers (1978), Ford (1988) and Ford and Williams (1989). Based on extensive field studies, they proved that the development of karst conduits proceeds along narrow joints and bedding planes. Ek (1970) studied the influence of bed-dips, joints and faults on karst morphology focusing on the role of fissures in determing the position and shape of most of the cave passages. With statistical approaches Lauritzen (1989) and Lauritzen et al. (1992) pointed out that shear faults and fissures are the most favourable discontinuities for the development of caves and endokarst hydrology. Solutional formation of caves is only possible where a pre-existing network of openings connects the recharge and discharge areas. Where joints are prominent, they can determine the pattern of nearly every passage in a cave (Palmer 1991). However, in most cavernous limestones only a few of the numerous initial fractures and bedding planes have been enlarged into cave passages. Thus there must be a strong preferential selection among these fractures for the available groundwater recharge (Groves & Howard 1994) and more research has yet to be done to understand this competitive processes operating between fractures.

Faults have been considered so far either to be obstacles in karst aquifers (e.g. Jeannin&Bitterli 1998) or to exert only local control on the development of cave passages; and consequently determine the overall trend of relatively few caves (Kastning 1977). In contrast to most of studies on karst development, which were carried out in synclines, platforms and monoclines, research conducted so far on anticline structures is rather rare (for terminology see Fig. 1). Huntoon (1993) point to the fact that anticlines contain large water systems with their own characteristic hydrogeology, which is closely related to tectonic structures. To close this gap in research, a better understanding of the function and interaction between tectonic structures and karst systems in anticlines must developed from well established tectonic models, which in turn will lead to more sound hydrogeological models.

The scope of the present study is to identify, localise and quantify the influence of tectonic structures, i.e. normal faulting, inverse faulting and tear joints on karst water flow patterns. In particular, the following issues will be addressed:

1) The significance and relative amount of water transport parallel to fold axes.
2) The role of synorogenic inverse faults as hydraulic barriers or preferred pathways.
3) The role of oblique normal faults as hydraulic barriers or lateral drainage system.
4) The existence and significance of hydraulic links between two separate karst aquifers.
5) The water transport through aquitards along faults.

In some parts of the Jura area a spatial coincidence between normal faults and occurrence of karst springs exists in anticlines (Herold 1997, Herold et al. 1997). Furthermore, long-distance groundwater transport parallel to anticline fold axes has been proved by many tracer tests (della Valle 1977, 1981).

Methods used in the present study

- Morphological and tectonically mapping.
- Hydrogeological mapping.
- An observation network of some 600 springs. The five largest springs were equipped with permanent sampling facilities to monitor discharge, temperature, and electric conductivity and oxygen stable isotope ratio. In the other springs, these parameters were collected periodically. Chemical and bacteriological analysis was also performed for a large number of springs.
- Three extended multi-tracer experiments (see below).
- Meteorological network which incorporated precipitation and oxygen stable isotope ratios.

Terminology used for tectonic structures

Folds occur in a variety of shapes and forms. In the brittle domain, folding is always associated with joints and faults (Fig. 1). Joints are extension cracks, which do not result in a

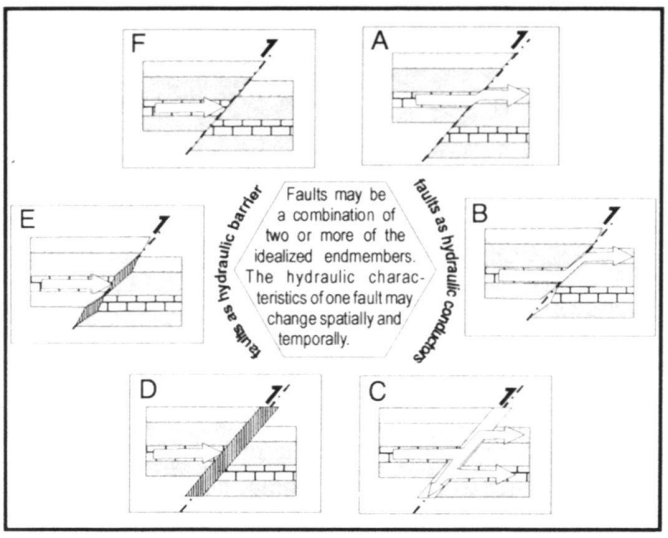

Fig. 2. Fault geometry and Karst conductibility: Depending on stress, strain and involved materials, three configurations may be distinguished: top) planar surface with no cavities; middle) irregular surface with cavities; and bottom) open joints or thrusts. In the first two cases, the joint or thrust does not act as potential aquifer, however it may cut (top left) or connect different potential aquifers by juxtaposition (top right). In the latter two cases, the openings may be filled by clay-like and thus impermeable materials ("fault gouge", left). Or they may be filled by sand-like fault breccias (middle right) or calcite veins (bottom right). These calcite veins my undergo karstification. Consequently, thrust may hinder (left) or promote karstification (right).

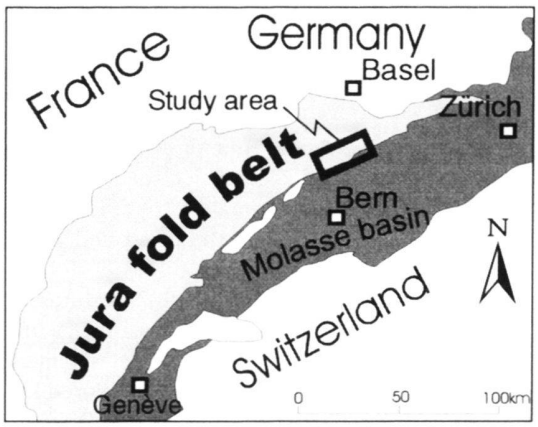

Fig. 3. Location of the study area.

measurable movement of the adjacent rock. In contrast, faults are fractures along which vertical (normal or reverse), lateral (strike-slip) or combined displacement (oblique-slip) occurs (Fig. 2).

2. Study area

To test the influence of tectonic structures on the formation of karst groundwater conduits in anticline structures, we chose the Weissenstein Anticline as one of the most typical Jura folds. The anticline is situated in the orogenically proximal part of the Eastern Jura fold-and-thrust belt (Fig. 3) and characterised by the following features which benefit the aims of the present research:

- It contains two regionally important karst aquifers separated and confined by thick low permeability strata which may be considered as aquitards or even aquicludes;
- Distinct recharge areas for both aquifers;
- A slightly plunging fold axis;
- A great number of joints and faults, normal as well as reversed, primary as well as reactivated;
- A sufficient number of karst water springs;
- Well defined hydrological boundaries and pre-existing data concerning geology, speleology (Arbenz 1999), hydrology and meteorology.

The study area is limited to the south by the Molasse Basin, to the East by the Oensingen Gorge (‚Klus of Balsthal') and to the West by the Weissenstein railway tunnel. The anticline axes correspond to the topographically higher areas, including the Weissenstein Anticline and the southern limb of the Farisberg Anticline. The hydrological closed Thal Valley occurs between the Weissenstein Anticline and the Farisberg Anticline. There is a significant difference between the calculated ground water recharge of the surface Thal Valley catchment area and the outflow (ground and surface water) at the Oensingen Gorge (Lüscher 1975, Herold 1997). The virtual excess of net precipitation compared to the total water discharge can be explained by:

1. An inaccurate definition of the catchment area, i.e. the surface watershed was used instead of the subsurface karst-drainage divide.
2. An incomplete measurement of discharge in the Oensingen Gorge, i.e. sub-surface sources or source by-pass was ignored or inaccurately estimated.
3. Existence of a trans-anticlinal drainage system discharching to the Gäu catchement.

In the past, many controversial hypotheses have been proposed to explain the tectonic evolution of the Jura Mountains. The thin-skinned Jura is part of the Alpine system and originates from late Miocene to Pliocene decollement of epi-Variscian sediments within the Triassic evaporites (Laubscher 1965, Jordan 1992). The Weissenstein Anticline and the Farisberg Anticline show complex structures resulting from a multiphase brittle deformation including Oligocene E-W rifting, early orogenic NW-SE directed thrusting and late orogenic NNW-SSE directed folding and thrusting. Though some aspects of kinematics and geometry are still disputed (Buxtorf 1907, Wiedemayer 1923, Laubscher & Pfirter 1984, Laubscher & Hauber 1982, Jamison 1987, Bitterli 1990), the main aspects can be summarised as follows (Herold 1997, Herold et al. 1997): SSW-NNE trending Oligocene normal faults were reac-

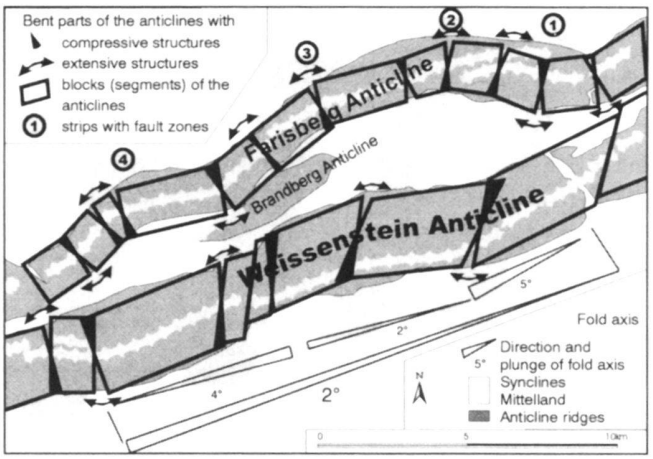

Fig. 4. Schematic diagram illustrating the division of the anticlines into single blocks (segments), which can be derived from the bending of the fold axis.

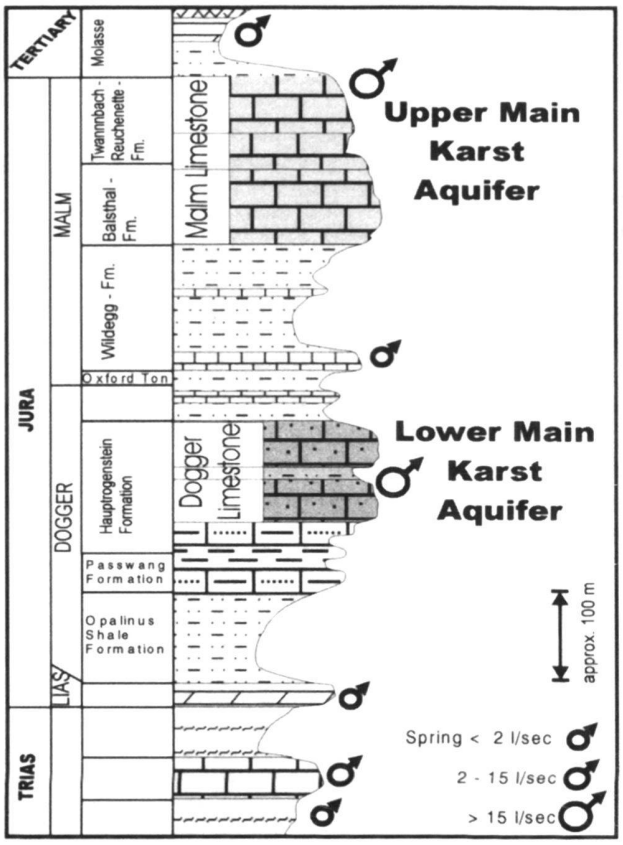

Fig. 5. Synoptic stratigraphic log, showing the main karst aquifers and spring levels.

tivated during Jura-Folding resulting in distinct change of fold axis strike and plunge. In the test area four distinct zones of discontinuity are distinguished (Fig. 4). In the convex part of fold axis bend, the reactivation was mainly transtensive, while transpressive reactivation occurred in the concave parts. Early-orogenic thrusts have been folded by lift-off-folding (e.g., Jamison 1987) followed by southerly trending asymmetric box folding (e.g., Laubscher & Hauber 1982), or southerly trending fault-propagation-folding (e.g., Bitterli 1990). Fold axes plunge is 1° to 5° (Fig. 4).

Five hydrogeological units can be distinguished in the test area (Fig. 5):

The first and lowest unit consists mainly of Middle Triassic to Early Middle Jurassic shales and marls altering with limestone and evaporite sequences.

The second unit is formed by the Mid-Jurassic Hauptrogenstein Formation, which consists of a 90-100m thick slab of oolithic limestone with subordinate shale interbedding (Gonzales & Wezel 1996). This unit forms the main lower karst aquifer in the interior of the anticlines. This aquifer derives its water solely from meteoric precipitation or infiltrating rivulets, which are fed by small springs on the crest, because it outcrops mainly at the top of the anticline. The outcrop area is characterised by a number of important dolines (up to 20m in diameter) and sinkholes. On the top of the anticline, karrenfields are covered with a thin soil layer. The karst groundwater flow and geomorphologic observations suggest an extensive and well-developed karst system. The Dogger Limestone in the Weissenstein Anticline is almost entirely drained by the Gerbiweiher Spring (Q_{mean}~ 15 l/sec, Q_{max}~ 500 l/sec) in the Oensingen Gorge.

The third unit (Late Middle Jurassic and Early Late Jurassic Marlstones) consists of a 200 m thick sequence dominated by marls and shales including some limestone. This unit acts as a low permeability seal separating the lower and upper main karst aquifer in the test area.

The fourth unit is the highly karstified Late Jurassic Malm Limestone. It is approx. 120m thick and consists of a broad variety of Late Jurassic fore-reef to back-reef sediments and some subordinate marlstone interlayer. An explored karst system in this unit the "Nidlenloch" system extends over 7.8 km (Glutz 1997). In contrast to the Dogger Limestone, the Malm Limestone outcrops on both limbs of the anticline, where it is exposed over a large area. A number of dry valleys occur on the limbs. Some of the valleys follow fracture zones trends. The Malm Limestones are mainly drained by three large karst springs, which are present at the base of the slope (Herold 1997, Herold et al. 1997):

- The Hammerrain Spring: Q_{mean}~ 22 l/sec, Q_{max}~ 30 l/sec.
- The Chaltbrunnen Spring: Q_{mean}~ 30 l/sec, Q_{max}~ 154 l/sec (An unknown proportion of the springs discharge flows into the adjacent gravel).
- The Hun Spring: Q_{mean}~ 71 l/sec, Q_{max}~ 1208 l/sec.

Few small ephemeral springs occur along the transition zone from the Malm to the Molasse in the valley. Some of the springs represent overflows from the karst systems. Additional diffuse outflowing water was observed in the deep valleys crossing the outcropping limestones during periods of higher karst water levels. Only a few very small springs discharge into the limbs or flow from the anticline crest and infiltrate in the limbs (diffusely or into sinkholes). Nevertheless, few dolines are present.

The fifth unit (Tertiary) occurs only in the valley between the main anticlines or in the Molasse Basin. It forms an impermeable layer from 0 to about 300 m thick.

3. Situation and Configuration of tracer test

The tracer tests were carried out based on an evaluation of favourable injection points as well as their possible connection to springs at the bases of the anticlines.

Initially, tectonic and geomorphologic structures, as well as the spatial distribution of karst systems were mapped in detail. All of the largest springs turned out to be connected to fault zones, or to gorges. Most of these springs upwell. Furthermore, the predominantly inactive Nidlenloch cave system in the northern limb of the Weissenstein Anticline was investigated. This system is only active during periods of high groundwater. It covers about 5% of the entire study area and is oriented along fracture systems perpendicular and parallel to the anticline axis.

Finally, the geological mapping as well as a seismic line shot along the valley show that four strips with local SW-NE fault sets cross diagonally the anticlines separating them into several segments (Fig. 4). These normal faults have been reactivated during Miocene folding in a transpressive or transtensive manner, due to rotation of the segments. Consequently, the strike of the slightly eastward dipping Weissenstein Anticline shows a s-shaped bend resulting from a broad dextral shear zone, confined by two pre-orogenic normal fault zones. In the transtensively influenced part of the limbs, large open fractures up to some meters wide have developed (Herold 1997, Herold 1997 et al.).

Based on these data and their interpretation, three tracer experiments were performed in 1994, 1995 and 1998 covering the whole study area. The tracers used (Käss 1998), include Eosin (Basacid red 316), Napthionate (Sodium-Napthionate), Lissamine (Direktgelb 96), Rhodamine (Sulforhodamin G (extra) Hoechst), Sulforhodamine (Duasyn-Säurerhodamin B 01), Pyranin (Pyranin 120%), Fluorescein (Fluorescein Natrium), Rhodamin WT (Acid red 388 CAS) and Duasyne (Duasyn-Fluoreszenzgelb-T Hoechst 26865). The tracers were injected into artificial trenches, sinkholes or dolines as well as diffusely infiltrating streams.

In 1994 tracers were injected at eleven different localities on the Weissenstein Anticline and Farisberg Anticline. A total of 58 springs were monitored during the test. In 1995, tests were carried out at eight injection points on the Weissenstein Anticline and 54 springs have been monitored. The predominantly dry weather conditions during the tracer tests were similar during the 1994 and 1995 test. In about 75 per cent of all examined springs and creeks, at least, one of the different tracers could be observed. In 1998 two additional tests have been performed in the north-eastern part of the Weissenstein Anticline.

3.1 Analytical methods

In order to quantitatively interpret the Weissenstein tracer experiments, Werner's (1998) software TRACI was used. For the interpretation of the tracer breakthrough curves the Multi-Dispersions-Model (MDM) was used (Maloszweski et al. 1992, 1994) with following settings: Porous aquifer: 1 dimension; Dirac-function: standardising; fit settings: method of moments; integral solution: Gauss-Legendre.

4. Results

In this paper only some selected and representative results (flow directions, flow velocity, recovery rate) are presented (Fig. 6, table 1). For a full overview we refer to Herold (1997). In Fig. 6 are the injection points marked with capitals and the relevant connections between injection and discharge point are numbered (see table 1).

The results of the tracer tests show obvious trends. Generally the main tracer flow direction is from W-SW to E-NE in both the Malm Limestone and the Dogger Limestone. This follows the general plunge of anticline axis. Subordinate flow directions can be observed in the opposite direction in the Malm Limestone, or along flow paths perpendicular to the anticline axis. Groundwater flows out of the surface water catchment. Often, an intersection of groundwater catchment is apparent. The Weissenstein Tunnel in the western part of the study area operates as an artificial drainage system. The highest flow velocities as well as highest recovery levels and relative concentration rates were observed in the areas surrounding the Oensingen-, Balsthal- and Gänsbrunnen Gorge. The Gerbiweiher Spring (Dogger Limestone) has the highest recovery level (up to 80%) and relative concentration. Tracer transport in water flowing along the fault zones generally had the lowest relative concentration and recovery rates (0.1%). The tracer injected in the Malm Limestone near Oensingen Gorge yielded the highest flow velocities (up to 2350 m/d, see point O in Fig. 6).

5. Discussion

Based on the tracer test results, three different flow systems may be distinguished:

- Karst groundwater flow in the external (Malm) limestone
- Karst groundwater flow in the internal (Dogger) limestone
- Karst water penetrating through the aquitards

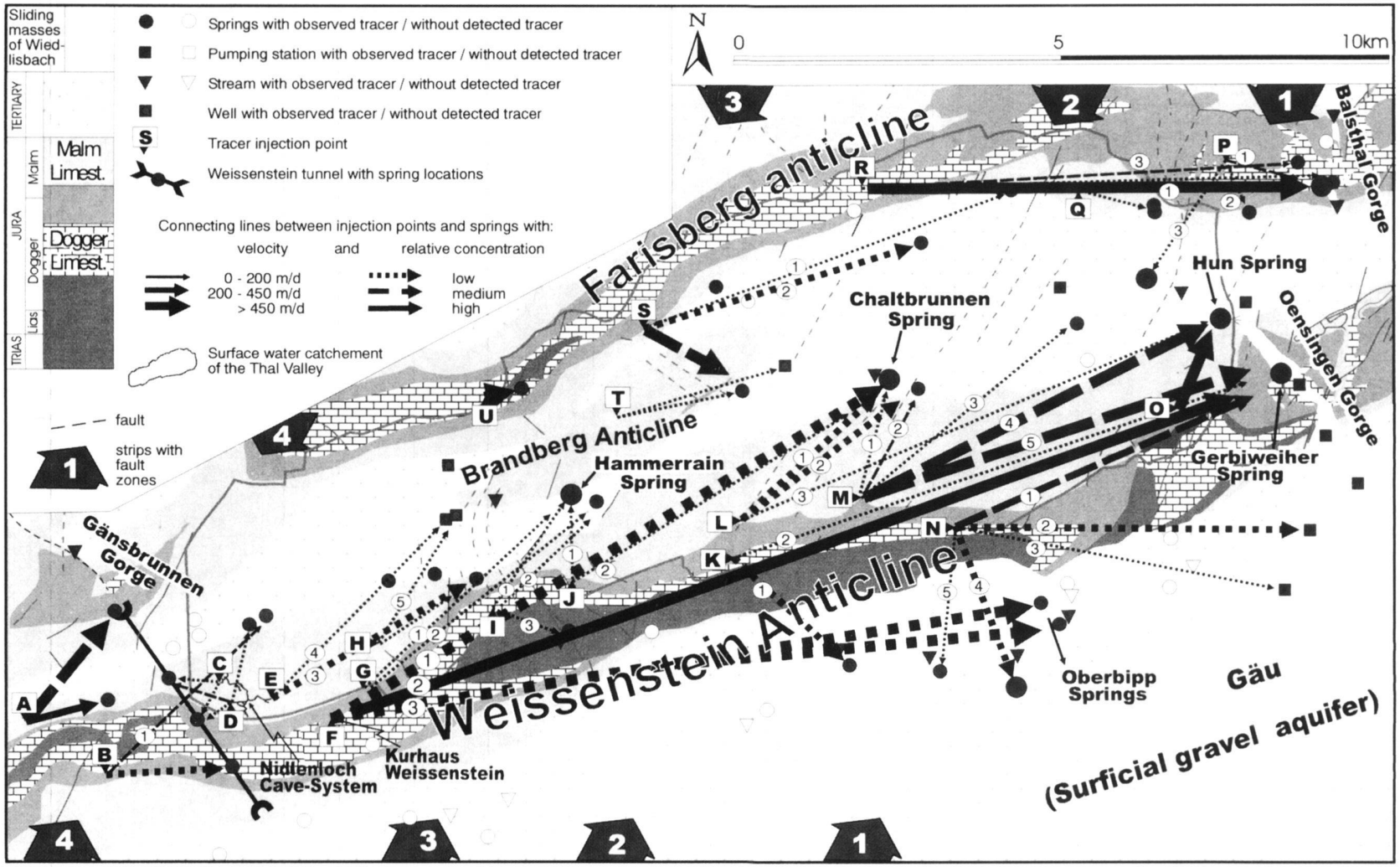

Fig. 6. Simplified geological map with the most relevant tracer results in the study area. The injection points are marked with capital letters. Connection lines (injection point to springs) mentioned in the text are numbered.

Tab. 1. Extract of the 1994 and 1995 tracer test results including all results discussed in the present paper. Numbers refer to Fig. 6. Observation time was 3 months in maximum. The water sampling was stopped after the measurement of the tracer breakthrough curves. For a full listing of all 119 positive and 44 negative correlations of 1994 and 1995 tests see Herold 1997.

A	x co-ordinate (spring)					F	First tracer arrival at the spring [d]					
B	y co-ordinate (spring)					G	Calculated mean flow velocity [m/d]					
C	Spring altitude [m]					H	Tracer injection quantity [kg]					
D	Connection between injection point and spring (see Fig. 6)					I	Max. measured tracer concentration [ppb] of a distinct breakthrough curve					
E	Distance between injection point and spring [m]					J	Tracer recovery rate [% of injected tracer]					
A		B		C	D	E	F	G	H	I	J	Year
603	850	234	850	770	B-1	3100	14	188	0.2	0.481		1994
606	900	235	860	740	E-1	3400	10	224	1.0	0.424		1995
606	375	235	840	750	E-2	3700	16	195	1.0	0.319		1995
607	175	235	805	780	E-3	4000	14	232	1.0	0.046		1995
606	675	236	400	680	E-4	4000	20	127	1.0	0.037		1995
606	890	236	530	675	E-5	4250	27	127	1.0	0.02		1995
606	875	236	560	675	E-6	4200	27	123	1.0	0.024		1995
613	825	238	675	500	F-1	10100	15	594	2.0	1.08	~1%	1995
614	826	239	676	500	F-1	10100	15	624	1.0	0.841	~1%	1994
619	695	238	760	480	F-2	15540	23	640	2.0	48.3	~50%	1995
619	695	238	760	480	F-2	15540	23	605	1.0	333.1	~80%	1994
616	310	234	880	530	F-3	11200	14	644	2.0	0.475		1995
616	085	235	310	630	F-3	11000	14	629	2.0	0.229		1995
609	901	237	931	600	G-1	4350	37	95	1.0	0.056		1994
609	550	236	990	580	G-2	4700	42	96	1.0	0.007		1995
606	900	235	860	740	H-1	1500	11	80	1.0	0.603		1995
606	375	235	840	750	H-2	1600	17	65	1.0	0.268		1995
607	175	235	805	780	H-3	1930	17	100	1.0	0.049		1995
606	675	236	400	680	H-4	2200	22	74	1.0	0.039		1995
606	890	236	530	675	H-5	2400	27	72	1.0	0.025		1995
606	875	236	560	675	H-6	2400	27	68	1.0	0.029		1995
608	900	236	930	600	I-1	2300	12	167	3.0	0.447	~0.2%	1995
609	550	236	990	580	I-2	2500	12	181	3.0	0.163		1994
608	710	234	570	810	I-3	1300	27	32.34	3.0	0.03		1995
608	700	234	500	800	I-3	1250	24	37	3.0	0.014		1995
608	900	236	930	600	J-1	1500	9	144	1.0	0.949	~1%	1995
613	825	238	675	500	J-2	6100	45	106	1.0	0.169	~0.1%	1995
613	50	234	100	610	K-1	2400	6	336	10.0	0.203		1995
613	825	238	675	500	L-1	3200	8	381	0.6	0.112	~1%	1994
614	750	238	700	504	L-2	3350	7	418	0.6	0.26		1994
618	820	239	600	480	L-3	8000	46	152	0.6	0.087	~8%	1994
613	825	238	675	500	M-1	1900	9	118	1.0	0.766		1995
614	750	238	700	504	M-2	1850	9	138	1.0	1.716		1995
616	675	239	725	520	M-3	4500	38	73	1.0	0.152		1995
618	820	239	600	480	M-4	6300	8	563	1.0	1.692	~20%	1995
619	695	238	760	480	M-5	6800	6	944	1.0	2.156	~6%	1995
619	695	238	760	480	N-1	5400	12	354	1.0	1.737	~10%	1995
620	005	236	60	460	N-2	5100	8	638	1.0	0.231		1995
619	825	235	425	460	N-3	5000	22	180	1.0	0.044		1995
615	810	233	815	490	N-4	2600	4	302	1.0	0.321		1995
614	345	234	130	600	N-5	2500	21	104	1.0	0.025		1995
620	370	241	625	515	P-1	1550	2	169	0.2	0.73		1994
619	340	241	235	580	P-2	950	15	53	0.2	0.086		1994
617	810	240	160	485	P-3	2200	19	110	0.2	0.064		1994
620	370	241	625	515	R-1	6950	14	454	0.2	10.16		1994
615	555	241	520	585	S-1	6000	42	130	0.5	0.142		1994
614	930	240	540	640	S-2	4450	15	230	0.5	0.215		1994

5.1 Tectonic structures as hydraulic pathways:

Folding and thrusting of the WSW-ENE trending anticlines was linked with the reactivation of the pre-existing SSW-NNE trending normal faults. Both resulted in the following hydrogeologically relevant structures:

- An overall trend of anticline fold structure with jointing parallel to the fold axis in the crestal parts of the anticlines (Fig. 1, A and B) and synorogenic conjungate shear system in the limbs (Fig. 1, C) is obvious.
- The horizontal bending of the fold axis is interpreted to be the result of the rotation of different fold segments (Fig. 4).
- The bending is concentrated along fault zones, which hydraulically confine the rotated blocks (Fig. 4, Fig. 1D). The fault zones act either as karst groundwater drainage conduits or appears to have no significant influence on karst water flow in the limbs parallel to the anticline axis.

The results of the tracer tests indicate that the above structures and tracer flow directions are related to groundwater flow conditions in the limestones as follows.

5.2 Karst groundwater flow in the external (Malm) limestone

Three different flow directions may be distinguished:

- A dominant trend from WSW to ENE parallel to the fold axes in the direction of axial plunge.
- Another trend from SSW to NNE or vice versa perpendicular to main flow direction related to the reactivated fault zones.
- A subordinate trend from ENE to WSW opposite to main flow direction. This last trend is observed in the vicinity of the Weissenstein tunnel (local drainage structure) and along a reactivated fault zone.

5.2.1 Axis-parallel flow in the blocks

None of the tracer tests performed in the limbs resulted in a maximum flow distance exceeding some 8 km although the whole length of the anticline is some 21 km. This is explained by the strong lateral drainage system (see below). Although alternative explanations like tracer-dilution caused by mixing groundwater systems or tracer-flow into karst systems with higher mean flow velocities cannot be fully excluded.

Regarding the tracer test results of one of the blocks in question, increasing flow velocity with distance can be revealed (Diagram in Fig. 7). Depending on where the discharge points occur, various positive relationships can be distinguished:

➢ The points on line 1 in the diagram of Fig. 7 represent outflows of the upper karst water level (spring I to III). This regime contrasts with the discharge pattern of the lower discharge points in Welschenrohr (line 2). The water discharging from the lower outlets probably flows through a less karstified system with a greater number of small fractures compared to water discharge from the upper springs.

The dominant flow direction parallel or sub-parallel to the fold axes is suggested to be related to extensional joints (A and B in Fig. 1), transtensively overprinted conjugate shear zones (C in Fig. 1) or opened fractures between single sedimentologic layers due to tectonic movement (Knez 1998).

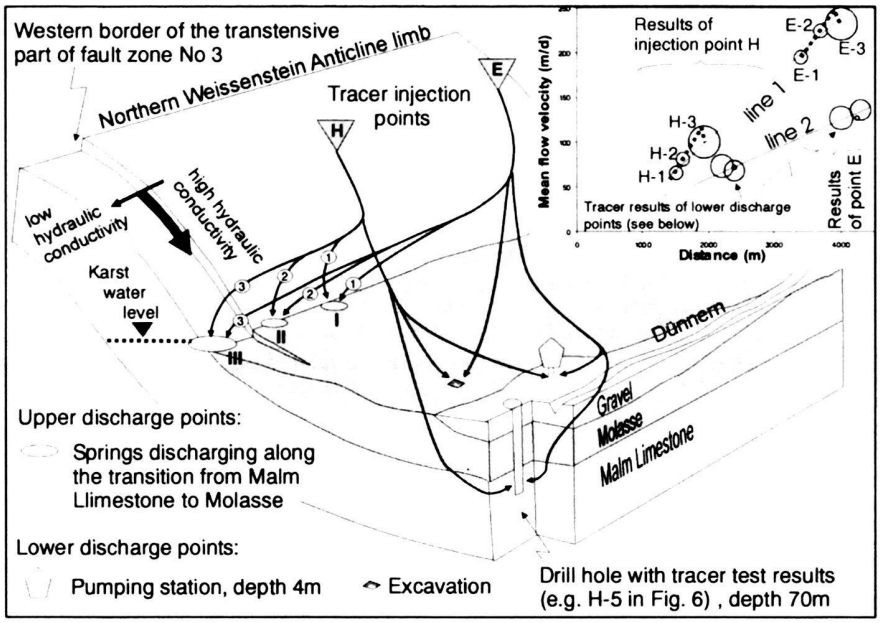

Fig. 7. Tracer results (see also Fig. 6) from the western part of the northern Weissenstein limb. The tracer at point E was injected into a stream flowing through the Nidlenloch Cave system; the tracer at point H was injected into an excavation on the northern limb. Generally, the flow velocity increases with distance (see diagram). For the last spring (H-3, E-3) of line 1 in the diagram, the water must pass the first significant lineament of fault zone 3 (see also E-3 in Fig. 6). This probably causes the slight offset (dashed lines) and reduced flow velocity of spring III compared to springs I (H-1, E-1) and II (H-2, E-2).

5.2.2 Local drainage along reactivated fault zones

As mentioned above, lateral flow in the fault zone never extend over the whole fold limbs. The flow is rather interrupted by reactivated Rhineish normal faults. These faults cut the anticlines in different rotated segments (Fig. 4) resulting in a horizontal bending of the fold axes. Due to this rotation, two different types of reactivation can be observed which results from the direction of block rotation:

- Transtensive reactivated fault zones with hydraulically transmissive fractures, perpendicular to the fold axis. These occur where the rotated blocks separate from each other.
- Transpressive fault zones with no influence on axis-parallel karst water flow in the Malm Limestone. These occur where the blocks converge together.

The transtensively reactivated fault zones are more deeply eroded than the adjacent limestones. Most of the groundwater in the Malm Limestone discharges from opened and widened fractures of the transtensive zones into large springs in the Thal Valley. We suggest that they mainly act as groundwater drainage conduits and drain most of the blocks' recharge between the fault zones. Due to this effect, maximum tracer flow distances of fast flowing karst water are significantly shorter (up to 8 km) compared to the Dogger Limestone (16 km, see below). However, the fault zones do not drain all of the recharge. A minor part obviously passes through the fault zones (Fig. 8) and discharge via springs further down gradient:

➢ The results of the 1994 test (L-3 in Fig. 6), where Sulforhodamin was injected into a sinkhole west of fault zone 2 are shown in Fig. 8 and 9. In 1995 the same tracer was injected into an infiltrating rivulet at the eastern margin of the same fault zone 2. The mean flow velocity and recovery rate in the latter tracer test (M-4) was clearly higher than in the 1994 test.

Due to the similar weather and infiltration conditions during 1994 and 1995 it is expected that the extensive fault zone between the two injection points L and M caused a significant decrease of flow velocity and concentration. These observations are confirmed by other tracer test results, such as S-2 and S-1 with comparable velocity differences or G-1 and J-2, which passed similar fault zones and which are situated on the same correlation line No. 2 in Fig. 9 as L-3 and S-1.

This observation can be explained by the fact that the transtensively reactivated faults induce offsets in the sedimentary layers. This is observed in the Grenchenberg Tunnel, 10 km west of Weissenstein Tunnel (Fig. 10). Consequently, three main factors decrease the flow velocity (Fig. 8): i) the water may have to change the flow direction abruptly; ii) the difference between the calculated distance between injection point and spring and the real distance increases with an increasing number of deflections; iii) velocity will change with fracture aperture. Increased aperture width will reduce flow velocity.

5.2.3 Water table in the Weissenstein Anticline outer limbs

We assume the water level in the Malm Limestone to be controlled by the largest springs, which discharge at the foot of the anticline. Due to the strong faulting in fault zone 3 and the simultaneous overthrusting of the Brandberg Anticline, which act as a sill, the Thal Valley is separated into a western (upper)

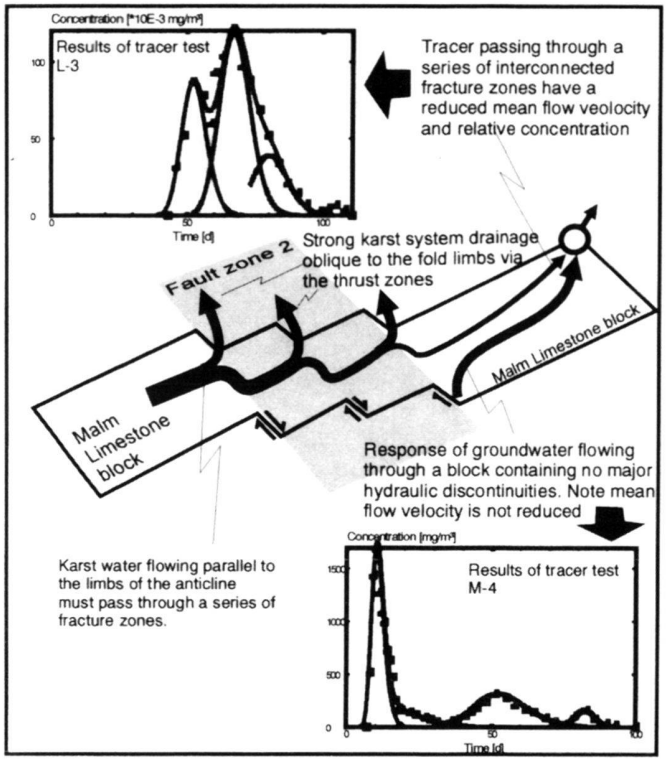

Fig. 8. Proposed conceptual model to explain reduced karst groundwater flow velocities. The model is derived from observed tectonic structures (see Fig. 10) and the results of the tracer experiments.

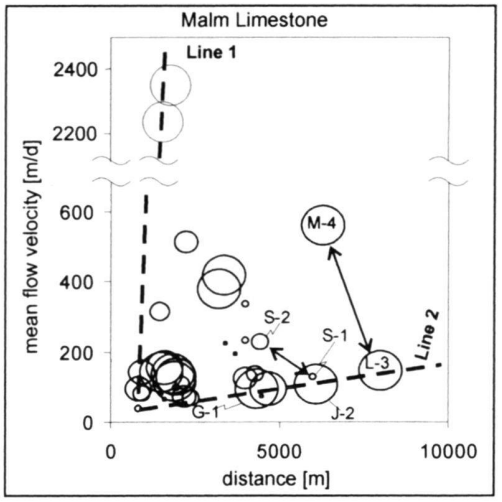

Fig. 9. Plot of mean flow velocity with distance for 1994, 1995 and 1998 tracer test results. The diagram shows a broad scatter of results with the largest distance up to 8 km from the injection point. No significant correlation is possible. Two lines define the range of velocity-distance relationships that may exist. Line 1 defines the maximum velocity-distance relationship. Line 2 defines the minimum. The highest velocities (approx. 2350 m/d) are observed below flow distances of 2500 m. At greater distances flow velocities do not exceed approx. 600 m/d.

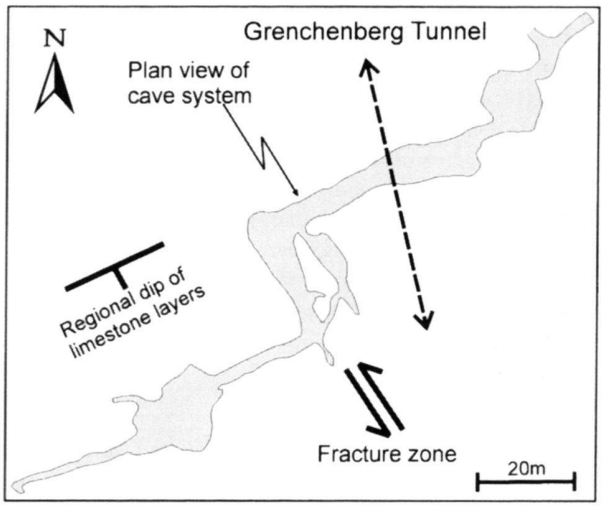

Fig. 10. Schematic plan view of a fault crossing the Grenchenberg Railway Tunnel. Along the displaced layer preferential groundwater flow occurs, resulting in offsets of the karst conduits.

and an eastern (lower) part. In the western part the karst water level is about 750 m AMSL and in the eastern part about 480 m AMSL.

5.3 Karst groundwater flow in internal (Dogger) limestone

The Dogger Limestone outcrops mainly along the anticline-crest. Our investigations show that the main karst water flow direction occurs parallel to the anticline over long distances. These systems have (Fig. 11):

- The longest flow distances (up to 16 km),
- The highest recovery rates (80%) and relative concentrations, and
- relatively high flow velocities (up to 623 m/d).

5.3.1 Deep groundwater system and local systems

The characteristics mentioned above were proved with the tracers F-2 and N-1 for the Weissenstein Anticline and R-1 or P-1 for the Farisberg Anticline. Such large and deep systems (regional systems) can be explained by the fact that impermeable layers bound the Dogger Limestone. Little water can escape laterally and it must therefore travel longer distances to the lowest drainage points in the Dogger Limestone (Gerbiweiher Spring in the Oensingen Gorge or the springs in the Balsthal Gorge). Additionally, the long distance transport is deduced from the folding related development of extensive joints parallel to fold axis (e.g. Fig. 1, A or B). The narrow range of results for the 1994 and 1995 test results at point F in the Dogger Limestones (F-2) and in the anticline limbs (F-1,

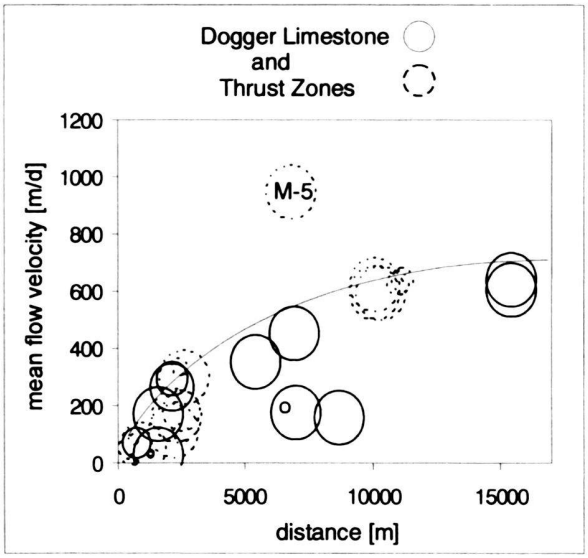

Fig. 11. Plot of mean flow velocity with distance for 1994, 1995 and 1998 tracer test results. Based on tracer test results, groundwater flowing in both the Dogger Limestone and along fault zones (between the anticline core and the limbs), flows with increasing velocity as distance increases, up to a maximum velocity of 600 m/d. One point is situated above the correlation line. It is the result of the tracer test, in which tracer flowed from the Malm Limestone into the Dogger (M-5, see Fig.6). It's high mean flow velocity can be attributed to different flow conditions (see 5.4).

F-3) give a mean flow velocity between 594 – 644 m/d. This indicates that groundwater velocities over this regional system are similar.

Karst water flow direction in the Dogger Limestone is influenced by the deepest discharge point (Gerbiweiher Spring) of the Dogger Limestone and an overall fold axis plunge of 2°. Local axes plunges in opposite direction to the general flow direction appear to have no influence.

The results of tracer tests at points F, I, K and N suggests much more complex, interfering Dogger Limestone karst systems (Fig. 6):

➢ Although most of the tracer at point F was recovered in the Gerbiweiher Spring, it does not drain all water infiltrating into the Dogger Limestone on the crest. Tracers injected at different places on the crest (points K and N) were not observed in Oberbipp Springs, although they were observed in some adjacent springs (K-1, N-4 and N-5) and at the Aare Gäu pumping stations (N-2 and N-3). An additional separate local catchment area exists at the intersection between the Weissenstein Anticline and fault zone 3. The tracer of point I, injected into the Dogger Limestone, appeared only in springs discharging in other strata to the north-east or south-east of the injection point.

We suggest that the observed flow patterns result from two different interfering groundwater systems in the Dogger Limestone. Evidence is as follows:

(a) A deep groundwater system (regional system) exists in the Dogger Limestone saturated zone as proved by the tracer test result at point F (F-2).
(b) Local systems along the crest of the anticline in the Dogger Limestone represent perched groundwater systems. They represent more superficial systems and drain part (point K, N) or all (point I) of the infiltrating water.

5.3.2 Main catchement area in the Weissenstein anticline

Due to the anticline fold geometry, the shape of the Dogger Limestone catchement is very long and narrow. For the Weissenstein Anticline the Oensingen Gorge acts as eastern boundary of the Dogger catchment area, with the Gerbiweiher Spring as the main discharge point. There are two catchement areas separated by overlying sediment but interconnected by the subsurface. The first and smaller catchement area is close to the Gerbiweiher Spring. The second and larger catchement area reaches as far as the Kurhaus Weissenstein (F-2). The Weissenstein Tunnel forms the western boundary of the catchment area. Eosin (point B) injected in the Dogger Limestone west of the Weissenstein Tunnel was observed only in the tunnel springs (Dogger Limestone).

5.3.3 Water table in the Weissenstein Anticline core

Water table elevations in the Dogger Weissenstein were estimated based on the following:

The lowest and largest discharge point in the Dogger Limestone is the Gerbiweiher Spring in the Oensingen Gorge. This spring drains most of the Dogger Limestone between the Oensingen Gorge in the East and the Weissenstein Kurhaus in the West. The Gerbiweiher spring water level (475 m AMSL) is assumed to be identical with the groundwater level of the karst system adjacent to the gorge.

Between the Gerbiweiher Spring and the western Oberbipp Springs, fold axis of the Dogger Limestone plunges relatively steeply (5°, see Fig. 4). This plunge reflects a significant rise of the Dogger Limestone fold axis that probably simultaneous cause an increase in the groundwater table elevation in the Dogger Limestone. This hypothesis is consistent with observations at the Oberbipp Springs:

➢ Eosin was injected into the Dogger Limestone regional groundwater system near Weissenstein Kurhaus (point F). Even before the tracer was observed in the Gerbiweiher Spring, it was observed in two other springs at Oberbipp (F-3), and in an adjacent rivulet beside them. Both springs are situated along the same NW-SE trending transtensive fault zone lineament. The highest spring is about 650 m AMSL. This is the highest point where the regional karst groundwater from the Dogger Limestone was detected.

We consider the elevation of the Oberbipp Springs as an indicator for the lowest water table in the Dogger Limestone regional groundwater system at this place.

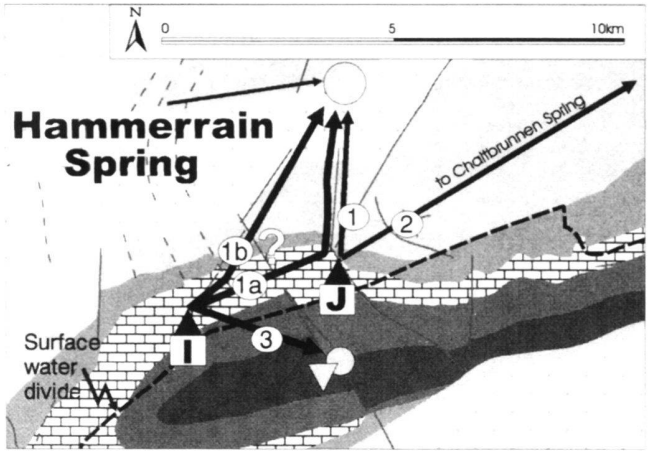

Fig. 12. Simplified tectonic sketch showing the results of the 1995 Pyranin and Fluorescein test in the vicinity of Hammerain Spring (see Fig. 6).

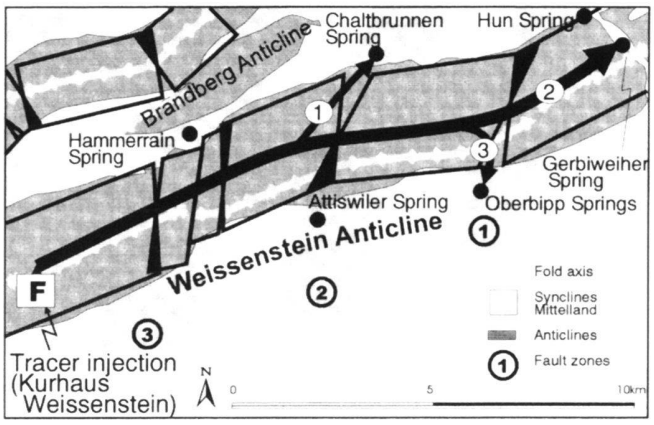

Fig. 13. The results of the 1995 Eosin test on a simplified tectonic sketch (see Fig. 4). The test, which definitively confirmed the earlier 1994 test, shows that the way in which a pre-existing fault zone has been reactivated determines whether the fault zone acts as a hydraulic barrier or as a hydraulic conduit. The tracer was injected some 100 m west of Weissenstein Kurhaus into the Dogger Limestone.

Further west, near the Kurhaus Weissenstein, no direct water table elevation information is available. Assuming that the fast karst water flow in the Dogger Limestone and the large discharge of the Gerbiweiher Spring indicate a well developed groundwater flow system that extends along the core of the anticline over a distance of 16 km, we suspect that the water level in the Dogger Limestone slightly increases between Oberbipp Springs and the Weissenstein Kurhaus

5.4 Aquitards zones penetrated by karst water

Although the two large karst aquifers of the Dogger- and Malm Limestone are separated by thick impermeable layers, the tracer tests show that hydraulic connections exists between both aquifers. It is the most likely that certain tectonic structures help to create flow paths penetrating these thick aquicludes, as:

- Direct contact of the two karst aquifers by juxtaposition (Fig. 2A).
- Hydraulic connections along fault planes (Fig. 2B, 2C).

5.4.1 Water flow from dogger aquifer to malm aquifer

Only at one place in the test field, the juxtaposition of the two main aquifers along reactivated Oligocene normal faults can be observed (Fig. 12):

➢ Fluoresceine (point J) was injected in 1995 into a creek, which infiltrate into this tectonic contact. The tracer was detected later in the northern Hammerrain Spring (J-1). The velocity (144 m/d) and the recovery rate (~1%) were relatively low. Simultaneously, the tracer Pyranin (point I) was flushed into a doline in the Dogger Limestone about 1.1 km west of point J and also observed in the same spring (I-1). The velocity (167 m/d) and the recovery rate (~0.2%) of this tracer test were in the same order as for point J.

It is possible that the tracer of point I flow from the Dogger Limestone into the Malm via this juxtaposition contact (I-1a). Alternatively, it is possible that it flowed along a WSW-NEN running lineament (I–1b) which direct connects the injection point and the Hammer Spring (Fig. 12). The significance of such fault initiated lineaments with no juxtaposition of the main karst aquifers is reflected by the I-3 results. The tracer was detected in two other springs, which discharge into the Muschelkalk limestone (a third aquifer far underneath and separated by thick aquicludes from the Dogger limestone), on the southern Weissenstein limb, on the other side of the surface water catchement. The only possible way to pass through all the intervening aquicludes is along hydraulically active fault zones.

Other tracer test results showed that the manner by which fault zones have been reactivated determines if the fault zones act as hydraulic barriers or as hydraulic conductive zone.

➢ Tracers were injected in 1994 (Fluorescein) and 1995 (Eosin) (point F in Fig. 6 and Fig. 13) into a sinkhole near Weissenstein Kurhaus in the Dogger Limestone of the Weissenstein Anticline. As expected from an earlier test, the first arrival of both tracers was observed after 23 days in the Gerbiweiher Spring (~16 km distance) within the Dogger Limestone of the Oensingen Gorge. The dispersivity is very low. About 80% (1994) or 50% (1995) of the tracers were recovered. However, the tracers were also observed in the Chaltbrunnen Spring in the Thal Valley (F-1, 10.1 km, 594 m/d). However, recovery rate for the Chaltbrunnen Spring was very low (~1%). It shows that a small portion of water passed from the interior of the anticline into the outer limb. The tracer was not found in other

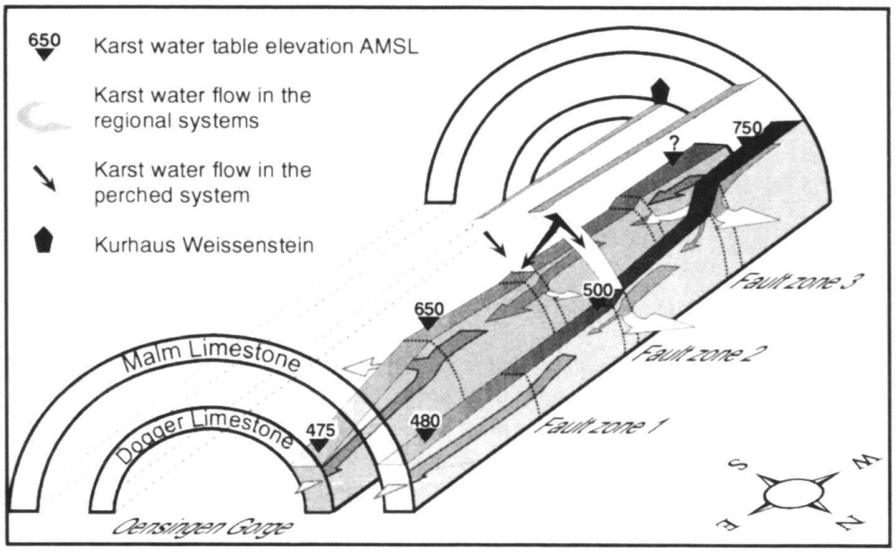

Fig. 14. A NE-SW schematic view of karst water circulation in the northern limb of the Weissenstein Anticline. Groundwater flow is restricted to the Malm and Dogger Limestone aquifers, the fault zone, related lateral drainage, results in a significant decrease of hydraulic heads. In the unsaturated zone water flow in the opposite direction can be observed along the fault zone.

springs neither in the northern limb nor elsewhere but in the Oberbipp Springs (F-3, 11 km, 629 m/d) discharging in the landslide mass covering the outer southern limb.

The results of the tracer test of point F matches very well with the model of rotated blocks (see above, Fig. 4 and Fig. 13).

This goes also for other tracers injected in the Dogger Limestone:

- In 1994 Sulforhodamin (point P) was injected into an infiltrating creek at the boundary of the Dogger Limestone and an impermeable layer. The tracer was observed in Dogger Limestone springs in the Balsthal Gorge (P-1) as well as in a spring in the Malm Limestone (P-2) and in a large upwelling spring in the Thal Valley (P-3). This latter spring discharges from the Molasse in a distance of about 1km from the Malm Limestone of the northern limb.
- In 1994 Eosin (point B), which was injected into the Dogger Limestone west of Weissenstein Tunnel, was observed in a Malm Limestone spring (B-1). The tracer was not observed in Malm springs in the Weissenstein Tunnel nor in other springs on the northern limb or elsewhere.

5.4.2 Opposite water flow from Malm to Dogger aquifer

Two test results show that the transtensively reactivated fault zones give way also for water penetrating the impermeable layers from the outer to the inner aquifer (Fig. 6):

- Tracers, Naphtionate (point C) and Lissamine (point D) injected in the Nidlenloch cave system (Malm Limestone) could be observed in Dogger springs of the Weissenstein Tunnel.
- Tracer injected at point M into a stream infiltrating into the northern limb of the Weissenstein (Malm Limestone) have been observed in springs in the Malm Limestone (M-1, M-2, M-3, M-4) as well as in the Gerbiweiher Spring in the Dogger Limestone (M-5).

The high velocity (Fig. 11) of the connection M-5 and its low dispersivity points to a hydraulically well developed system. As the tracer was injected in a tectonically transtensive zone, it is very probable that water flows from the limbs into the interior of the anticline along open fracture zones which are highly conductive.

Furthermore, hydrological calculations for the Weissenstein Anticline suggest that more water flows from the limbs into the interior of the anticline as in the opposite direction (Herold 1997). The calculated discharge of the Gerbiweiher Spring, which drains the Dogger Limestone of the whole Weissenstein Anticline, is too high for the assigned recharge area. In contrast, the discharge of the Hammerrain Spring, which drains the limbs of the western part of Malm Limestone, is too low for the assigned recharge area. Probably, water flows from the Malm Limestone (Hammerrain recharge area) into the Dogger Limestone (Gerbiweiher recharge area) along transtensively reactivated parts of fault zone 3.

5.4.3 Groundwater flow in the saturated and unsaturated Zone

As outlined previously the water level of the saturated zone in the western part of the of Dogger Limestone is about 650 m AMSL and in the Oensingen Gorge about 475 m AMSL. Compared with that, the water level in the Malm Limestone of the northern Weissenstein limb is higher in the western part and lower in the middle part of the anticline (Fig. 14). Along the northern limb of the anticline, only the transtensively opened fault zones 2 and 3 enable a pathway for water flow between the two main aquifers (Fig.13). These observations and the associated hypothesis imply connected regional karst water

systems exist in the saturated zone along transtensivly opened fault zones from W to E as follows:

- Hydraulic gradient penetrates along fault zone 3 from the Malm Limestone into the Dogger Limestone (indicated by result of water balances).
- In about 6 km east of fault zone 3, the water flows from the Dogger Limestone into the Malm via fault zone 2 (proved by tracer test result F-1).

Conversely, water flow in the opposite direction was proved by two simultaneous tests:

- A first transfer occurs along fault zone 3 from the Dogger Limestone into the Malm Limestone (I-1, I-2).
- In the eastern fault zone 2, the tracer was injected at point M into an infiltrating stream. This stream is suspected to bifurcate into both, the Dogger (M-5) and the Malm Limestone karst systems (M-1, M-2, M-3 and M-4).

The cross formational flow indication discussed above show that two separate groundwater systems, one in the regional groundwater system and a perched system in the unsaturated zone, exist. Groundwater is believed to flow between the Dogger Limestone and the Malm Limestone in both of these systems. This makes it possible for the water to cross in both direction the aquiclude along the same fault zone. For example, groundwater flow through fault zone 2 discharges from the Dogger Limestone to the Malm Limestone in the regional groundwater system (F-1). Conversely, water flows through the same fault zone in the opposite direction in the perched system (M-5).

The possibility of water flow through aquitards along fault zones can be explained by following hypothesis. After opening of large voids, the impermeable layers were partially filled with (fibrous) calcite. In this way the voids were not closed by clay swelling. Later, most or a part of the calcite was dissolved by karstification processes. However, it may not be excluded that the hydraulic pathways through the impermeable layers are a result of porous cataclasites, which were formed during the transtensive reactivation of the pre-orogenetic fault zones.

6. Conclusion

Our Studies on the Weissenstein- and Farisberg Anticline included a broad range of field mapping techniques (e.g. spring discharge and water quality monitoring and multi-tracing). Data collected using these methods provided a better understanding of the relationship between karst system flow patterns and orogenic structures. Though apparently rather unsystematic or even chaotic, the karst development and groundwater circulation scheme turned out to be highly dependent on rock anisotropy that resulting from Jurassic sedimentation, Oligocene normal faulting and Late Miocene Jura folding, including reactivation of the inherited structures. The study's most pertinent results may be summarised as follows:

- Fast long distance ground water circulation parallel to fold axes in the crest and limb regions of anticlines is not only a typical pattern of the study area but of Central Jura.
- This long distance transport, which is highly unfavourable from a hydraulic point of view, (generally, potential drainage points at comparable elevations as the yet active ones are abundant at much closer distances) is due to the folding related development of extensive joints parallel to fold axis. As most of the Jura folds have developed as fault-propagation folds, such extensive joints are also abundant in limb regions. Thus it may be concluded that the flow direction is controlled by overall axial plunge rather than by the local axial plunge or by the inclination of strata.
- Crossing pre-orogenic normal faults interrupt the axis parallel flow. Interestingly, only transtensively reactivated faults act as lateral drainage systems while transpressive reactivation seems to be unfavourable to karst development. Transtensively reactivated normal faults also result in hydraulic short-cuts connecting inner and outer aquifers. The direction of water transport, which may be 'in' or 'out', is on the one hand controlled by the two main aquifers' hydraulic heads, which vary spatially and temporally and, on the other hand by the occurrence of purged groundwater systems.
- Water flow through aquicludes at tectonic caused singularities, though not significant in quantity, seems to be as fast as water transport in most karst-aquifers. This fact needs explanation. Though these transtensive normal faults penetrating the Late Middle to Early Upper Jurassic marl and clay stones are not directly observable, we suggest that thick presumably fibrous calcite joints, which in turn have been subject to partial karstification, must penetrate through them. Thus, a hydraulic interconnection has been developed between the Dogger and Malm Limestones. Alternatively, it may be postulate, that transtensive reactivation results in porous cataclasites. However swelling of clay minerals would have reduced the permeability of these cataclastic fault zones.
- Folding related overthrusts or synorogenic conjungated shear systems cause joints, which function as potential connected openings for karst water flow. The flow velocity in these lateral drainage systems is very high and goes up to 2.3 km per day as it was proved for the outer aquifer.
- Additionally we can say that the draining effect of the gorges strongly influenced karst system development, though high karst maturity is observable in the closer surrounding of the gorges or even in systems which are directly connected to the gorges. This is reflected in a generally increasing trend of flow velocity and tracer recovery from the gorges to upper reaches of the valley.

Acknowledgements

This work was supported by the Swiss National Science Foundation (project 21-50733.97) and the Guillaume Foundation. The analysis of the tracers was done at Otz Laboratory in Bellmund (CH). We sincerely thank H. Otz for the analysis of tracers and Ray Flynn for english corrections. The careful reviews by Werner Balderer and Peter Huggenberger are greatly acknowledged.

REFERENCES

ARBENZ, TH. 1999: Speleoclub Neopyr Thal – Speleolgic data base. Unpublished, Matzendorf-Switzerland

BITTERLI, TH. 1990: The kinematic evolution of a classical Jura fold: a reinterpretation based on 3-dimensional balancing techniques (Weissenstein Anticline, Jura Mountains, Switzerland). Eclogea geol. Helv. 83/3, 493–512.

BUXTORF, A. 1907: Zur Tektonik des Kettenjura; Ber. Versamml. Oberrh. Geol. Ges., 40. Versammlung, 29–38.

DELLA VALLE, G. 1977: Hydrogéologie de la Vallé de Tavannes. Office de l'économie hydraulique et énergétique du canton de Berne (OEHE).

– 1981: Hydrogéologie du Vallon de St-Imier. Office de l'économie hydraulique et énergétique du canton de Berne (OEHE).

EK, C. 1970: Les influences structurales sur la morphologie de la grotte de Remounchamps (Belgique). Ann. Soc. Géol. Belgique 93/II, 293–304, Liège.

FORD, D. C. 1988: Characteristics of dissolution cave systems in carbonate rocks, in Paleokarst, edited by N. P. JAMES & P. W. CHOQUETTE, Springer Verlag, New York.

FORD, D. C. & EWERS, R. O. 1978: The development of limestone caves in the dimensions of length and depth, Can. J. Earth Sci., 15, 1783–1798.

FORD, D. C. & WILLIAMS, P. W. 1989: Karst Geomorphology and Hydrogeology, Unwin Hyman, Boston, Mass.

GLUTZ, R. 1997: Nidlenloch – aktueller Stand in Administration und Forschung. Akten des 10 Nationalen Kongresses für Höhlenforschung, Breitenbach/Schweiz, 6.–8. Oktober 1995. Ergänzungsband Nr. 14 zu «Stalactite», 98–101.

GONZALEZ, R. & WETZEL, A. 1996: Stratigraphy and paleogeography of the "Hauptrogenstein" and its basinal equivalent (middle Bajocian to middle Bathonian), northern Switzerland. Eclogae geol. Helv. 89.

GROVES, C. G. & HOWARD, A. D. 1994: Early development of karst systems, 1, Preferential flow paths enlargement under laminar flow, Water Resour. Res., 30(10), 2837–2846.

HEROLD TH. 1997: Grundwasser, Karstsysteme und tektonische Strukturen im Gebiet der Weissenstein- und Farisbergkette. Dissertation ETH-Zürich. Publikation Amt für Wasserwirtschaft, Kanton Solothurn.

HEROLD TH., BALDERER W. & JORDAN P. 1997: Hydrogeological investigations of the karstic system within the tectonically complicated part of the Jura-Region of the Canton Solothurn, Switzerland. In GÜNAY AND JOHNSON, A., editors, in Karst Waters and Environmental Impacts, Balkema, Rotterdam 1997, ISBN 9054105854, pp: 451–456.

HEROLD TH., BALDERER W. & JORDAN P. 1997: The influence of pre-existing and orogenetic faults on structures of modern groundwater circulation of two karstic aquifers in the southernmost anticline (Weissenstein) of the folded Jura (Switzerland). In: P.Y. JEANNIN, M. SAUTER Ed. Proc. Of 6th Conference on Limestone Hydrology and Fissured Medium, 10–17 Aug. 1997, La Chaux de Fonds, Switzerland.

HUNTOON, P. W. 1993: The influence of Laramide foreland structures on modern ground-water circulation in Wyoming artesian basins. In: Geology of Wyoming (Ed. by SNOKE, A.W., STEIDTMANN, J.R. & ROBERTS, S.M.) Geological Survey of Wyoming Memoir No. 5, p. 756–789.

JAMISON, W.R. 1987: Geometric analyses of fold development in overthrust terranes. J. of Struct. Geol. 9/2, 207–219.

JEANNIN P. -Y. & BITTERLI, TH. 1998: Speleogenesis of the north of Lake Thun cave system (Canton Bern, Switzerland): adequacy check between models and reality. Bulletin d'Hydrogéologie, Modelling in karst systems, special issue No. 16, Neuchâtel.

JORDAN, P. 1992: Evidence for large-scale decoupling in the Triassic evaporites of Northern Switzerland: an overview. Eclogae geol. Helv. 85, 677–693.

KASTNING, E. H. 1977: Faults as positive and negative influences on groundwater flow and conduit enlargement. Hydraulics problems in karst regions. Ed. R. DILAMATER, S. CSALLARY. Western Kentucky Univ.

KÄSS, W. 1998: Tracing Technique in Geohydrology. A. A. Balkema / Rotterdam / Brookfield / 1998, ISBN 9054104449.

KIRALY, L. 1968: Éléments struturaux et alignement de phénomènes karstiques. Bull. Soc. Neuchât. Sciences Nat. 91.

KIRALY, L., MATHEY, B. & TRIPET, J-P. 1971: Fissuration et orientation des cavités souterraines. Rögion de la Grotte du Milandre (Jura Tabulaire). Bull. De la Société Neuchâteloise des Sciences Naturelles, Tome 94.

KNEZ, M. 1998: The influence of bedding planes on the development of karst caves (a study of Velika Dolina at Skocjanske Jame Caves, Slovenia). Carbonates and Evaporites, 13/2, 121–131.

LAUBSCHER, H. & HAUBER, L. 1982: Querschnitt durch das Juragebirge zwischen Oensingen und Basel: Jber. Mitt. Oberrh. Geol. Ver. N.F. 64, 73–77.

LAUBSCHER, H. & PFIRTER, U. 1984: Bericht über die Exkursion der Schweizerischen Geologischen Gesellschaft in den östlichen Faltenjura, vom 15. bis 17. Oktober 1983. Eclogae geol. Helv. 77/1, 205–219.

LAUBSCHER, H. 1965: Ein kinematisches Modell der Jurafaltung, Eclogea geol. Helv. 58/1, 231–318.

LAURITZEN, S.E. 1989: Shear, tension or both – a critical view on the prediction for caves.– Proc. X intern. Cong Speleology, 118–120, Budapest.

LAURITZEN, S.E., OLDING, N. & PETERSEN, J. 1992: Modelling the evolution of channel networks in carbonate rocks. Eurock'92. Thomas Telford, 57–63, London.

LÜSCHER, P. 1975: Beiträge zur Hydrometeorologie und Hydrologie des Dünnerntals (Solothurnerjura) Dissertation Universität Bern, Zibo Druck Bottmingen.

MALOSZEWSKI P. 1992: Mathematical modelling of tracer experiments in the Karst of Lurbach System. Steir. Beitr. Hydrogeol. 43, 116–143.

– 1994: Mathematical modelling of tracer experiments in fissured aquifers. Freiburger Schr. Hydrologie, 2, 107.

PALMER A.N. 1975: The origin of maze caves: National Speleological Society Bulletin, V. 37, 56–76.

– 1991: The origin and morphology of limestone caves, Geol. Soc. Am. Bull., 103, 1–21.

RAMSAY, J. G. & HUBER, M. I. 1983: The Techniques of Modern Structural Geology. Vol. 2. Academic Press. London.

SNOW, D. T. 1969: Anisotropic permeability of fractured media. Water Resour. Res. 5/6, 1273–1289.

WERNER, A. 1998: TRACI - An example for mathematical tracing-interpretation-model. Tracing Technique in Geohydrology (Ed. by W. KÄSS). Balkema. 377–379.

WIEDENMAYER, C. 1923: Geologie der Juraketten zwischen Balsthal und Wangen a. A. Beitr. geol. Karte der Schweiz N. F. 48.

Manuscript received February 18, 2000
Revision accepted September 29, 2000